MOLECULAR ECOLOGY

Molecular Ecology (2015) **24**, 5495–5506 doi: 10.1111/mec.13396

Population genetic structure of a common host predicts the spread of white-nose syndrome, an emerging infectious disease in bats

ARYN P. WILDER, THOMAS H. KUNZ and MICHAEL D. SORENSON
Department of Biology, Boston University, 5 Cummington Mall, Boston, MA 02215, USA

Abstract

Landscape complexity influences patterns of animal dispersal, which in turn may affect both gene flow and the spread of pathogens. White-nose syndrome (WNS) is an introduced fungal disease that has spread rapidly throughout eastern North America, causing massive mortality in bat populations. We tested for a relationship between the population genetic structure of the most common host, the little brown myotis (*Myotis lucifugus*), and the geographic spread of WNS to date by evaluating logistic regression models of WNS risk among hibernating colonies in eastern North America. We hypothesized that risk of WNS to susceptible host colonies should increase with both geographic proximity and genetic similarity, reflecting historical connectivity, to infected colonies. Consistent with this hypothesis, inclusion of genetic distance between infected and susceptible colonies significantly improved models of disease spread, capturing heterogeneity in the spatial expansion of WNS despite low levels of genetic differentiation among eastern populations. Expanding our genetic analysis to the continental range of little brown myotis reveals strongly contrasting patterns of population structure between eastern and western North America. Genetic structure increases markedly moving westward into the northern Great Plains, beyond the current distribution of WNS. In western North America, genetic differentiation of geographically proximate populations often exceeds levels observed across the entire eastern region, suggesting infrequent and/or locally restricted dispersal, and thus relatively limited opportunities for pathogen introduction in western North America. Taken together, our analyses suggest a possibly slower future rate of spread of the WNS pathogen, at least as mediated by little brown myotis.

Keywords: emerging infectious disease, fungal pathogen, population genetic structure, RAD-seq, white-nose syndrome

Received 18 February 2015; revision received 18 September 2015; accepted 21 September 2015

Introduction

The spatial spread of emerging infectious diseases is shaped in part by complex landscapes, which influence host dispersal and in turn the genetic structure of host populations. The geographic structure of genetic variation in hosts and pathogens can thus shed light on disease dynamics across space and time (Archie *et al.* 2009; Biek & Real 2010). Genetic variation in pathogens has been used to reveal sources of infection, reservoir hosts or refugia (Girard *et al.* 2004; Rambaut *et al.* 2008), as well as invasion and spatial diffusion dynamics (Holmes 2004; Biek *et al.* 2007; Tian *et al.* 2015). Less commonly, population genetics has been used to measure the connectivity of host populations over heterogeneous landscapes to understand rates and routes of host-mediated pathogen dispersal (Blanchong *et al.* 2008; Rioux Paquette *et al.* 2014). We assessed host population genetic structure to test whether historical patterns of connectivity and gene flow are correlated with the spatial spread to date of white-nose syndrome

Correspondence: Aryn P. Wilder, Fax: +1 (617) 353 6340;
E-mail: apw@bu.edu

© 2015 John Wiley & Sons Ltd

1365294x, 2015, 22, Downloaded from https://onlinelibrary.wiley.com/doi/10.1111/mec.13396, Wiley Online Library on [19/11/2022]. See the Terms and Conditions (https://onlinelibrary.wiley.com/terms-and-conditions) on Wiley Online Library for rules of use; OA articles are governed by the applicable Creative Commons License

(WNS), an emerging infectious disease of hibernating bats.

WNS is a disease of North American bats that first emerged in 2006 in a hibernaculum near Albany, New York (Blehert *et al.* 2009). Available evidence suggests that WNS is one of a growing list of emerging infectious diseases caused by exotic pathogens (Puechmaille *et al.* 2011; Warnecke *et al.* 2012) with detrimental effects to native species (Daszak *et al.* 2000). WNS is caused by the fungal pathogen *Pseudogymnoascus destructans*, which grows maximally at temperatures characteristic of bat hibernacula (Lorch *et al.* 2011; Verant *et al.* 2012; Minnis & Lindner 2013). Transmission of *P. destructans* occurs through direct contact between infected and susceptible bats (Lorch *et al.* 2011), with infection prevalence highest during the hibernation season (Langwig *et al.* 2015). Following its emergence, WNS spread rapidly throughout eastern North America, causing massive mortality in several bat species, leading to predictions of regional extinction for at least two species (Frick *et al.* 2010; Langwig *et al.* 2012; Thogmartin *et al.* 2013). WNS continues to spread, extending into southern Canada, southward to Mississippi, and as far west as eastern Oklahoma, reaching locations over 1800 km from the epicentre in New York (USFWS 2015).

The spread of WNS across the landscape has not followed a simple diffusion pattern from its site of origin in North America (Maher *et al.* 2012). For example, WNS appeared as far south as southern Virginia before it reached the western edge of New York. Previous analyses indicate that colony size, species composition, habitat patchiness and climate influence WNS risk and consequently the overall pattern of spread across the landscape (Wilder *et al.* 2011; Maher *et al.* 2012; Thogmartin *et al.* 2012). Ultimately, spatial expansion of an infectious disease depends on pathogen dispersal, which, for pathogens transmitted directly between hosts, depends in turn on the connectivity of host populations. If bats are the primary mode of dispersal for *P. destructans*, then introduction of the fungal pathogen and risk of WNS to susceptible colonies should be a function of dispersal of bats from infected to susceptible winter colonies. Geographic distance to an infected colony is known to be negatively correlated with the timing of WNS arrival at susceptible colonies (Wilder *et al.* 2011; Thogmartin *et al.* 2012). Additional heterogeneity in pathogen dispersal may exist as a result of barriers to and/or corridors for host dispersal, which should be reflected in patterns of host population genetic structure. Therefore, we hypothesized that the probability of WNS infection would decrease with increasing genetic differentiation between susceptible and infected colonies.

The common and wide-ranging little brown myotis (*Myotis lucifugus*) is among the most severely affected and thoroughly studied WNS host species. While it is just one of several bat species affected by WNS, little brown myotis is likely the most important disperser of *P. destructans* over the landscape relative to other species due to its high abundance and dense aggregation in hibernacula (Brack 2007; Wilder *et al.* 2011; Langwig *et al.* 2012), high rate of infection by *P. destructans* (Langwig *et al.* 2015) and long dispersal distances (Davis & Hitchcock 1965; Humphrey & Cope 1976; Norquay *et al.* 2013); the number of little brown myotis in mixed-species hibernacula is positively associated with WNS risk to the colony (Wilder *et al.* 2011). In Pennsylvania, three hibernating colonies of little brown myotis that had higher levels of differentiation in mitochondrial DNA (mtDNA) haplotype frequencies also became WNS positive later than other colonies (Miller-Butterworth *et al.* 2014). This observation lends some support to the hypothesis that barriers to gene flow in little brown myotis may slow the spread of WNS. In this study, we quantitatively test for a relationship between population genetic structure among hibernating colonies of little brown myotis and the spatial spread of WNS in eastern North America, predicting that the inclusion of genetic data in models with geographic distance will significantly improve the estimates of WNS risk to susceptible colonies as compared to models with geographic distance alone. We then present data on the population genetic structure of little brown myotis on a continental scale to qualitatively assess the potential for future spread of WNS across the continent. We used mtDNA and double-digest, restriction site-associated DNA sequencing (ddRAD-seq; Baird *et al.* 2008; DaCosta & Sorenson 2014), which generates data from thousands of loci scattered throughout the genome. Our work illustrates that genetic analysis of host populations can identify cryptic barriers and/or corridors to dispersal and heterogeneity in population connectivity that may strongly influence disease spread, allowing a prospective assessment of the permeability of populations to pathogen invasion and improving predictions of the future dynamics of emerging infectious diseases.

Materials and methods

Sample collection

To evaluate the relationship between host population genetic structure and the spread of WNS, we obtained tissue samples (heart muscle, pectoral muscle or wing membrane) from 128 little brown myotis captured at 14 hibernacula located within the current distribution of WNS in eastern North America between the months of

© 2015 John Wiley & Sons Ltd

1365294x, 2015, 22, Downloaded from https://onlinelibrary.wiley.com/doi/10.1111/mec.13396, Wiley Online Library on [19/11/2022]. See the Terms and Conditions (https://onlinelibrary.wiley.com/terms-and-conditions) on Wiley Online Library for rules of use; OA articles are governed by the applicable Creative Commons License

September and April in 2008–2010. At each hibernaculum, between 2 and 14 (Table S1, Supporting information) individual bats were sampled prior to or at the onset of die-offs from WNS and thus are representative of populations in the pre-WNS period.

For a continental, rangewide assessment of population genetic structure in little brown myotis, we obtained tissue samples from a total of 599 bats collected at 71 maternity colonies, swarming sites, hibernating colonies or foraging sites across North America (Table S1, Supporting information); all samples were collected prior to or at the onset of die-offs from WNS. Tissues were obtained from previously collected tissues archived at Boston University, from natural history museums and other research institutes, from other workers conducting research in the field and through our own fieldwork. All bats captured through our fieldwork were handled using methods approved by the Institutional Animal Care and Use Committee at Boston University (Protocols 10-032 and 13-041). DNA was extracted using the DNeasy Blood and Tissue Kit (QIAGEN, Hilden, Germany).

Population genetic structure

To evaluate continental patterns of population genetic structure for a maternally inherited marker, we sequenced 536 bp of the mitochondrial cytochrome *b* (cyt*b*) gene for 557 individuals from 68 sampling sites. Cyt*b* primers L15524 (5′-ACRGGRTCYAACAAYCCAA CAGG-3′) and H16064 (5′-TCCCCTTTTCTGGTTTA CAAGACC-3′) were used to amplify and sequence a portion of the cyt*b* locus using a standard touchdown PCR protocol (Balakrishnan & Sorenson 2007). PCR products were sequenced from the forward primer on an ABI PRISM 3100 sequencer. A haplotype network was constructed from a maximum parsimony tree generated in PAUP (Swofford 2002); additional *Myotis* sequences from GenBank were included as out-groups in the phylogenetic analysis.

We also used a ddRAD-seq protocol developed by DaCosta & Sorenson (2014) to generate genomewide sequence data for 308 bats from 58 sampling sites. Genomic DNA was digested with *Sbf*I and *Eco*RI restriction enzymes (New England Biolabs, Ipswich, MA, USA). Amplification and sequencing adapters, each with a unique barcode or index sequence, were ligated onto the digested DNA. Samples were run on a 2% agarose gel, and DNA in the 300–450 bp size range (178–328 bp excluding adapters) was excised from the gel and amplified with 22 cycles using Phusion High-Fidelity DNA Polymerase (Thermo Scientific, Waltham, MA, USA). Each sample library was pooled in equimolar amounts and sequenced to 97 bp from the *Sbf*I adapter on an Illumina HiSeq 2000 or HiSeq 2500 (Illumina, San Diego, CA, USA).

Sequences that passed the Illumina quality filter were parsed into samples based on barcode and index sequences, and identical sequence reads within each sample were condensed, retaining the number of observations of each unique sequence as a weight for downstream analysis (DaCosta & Sorenson 2014). Data for all samples were pooled and clustered into putative loci using the UCLUST method in USEARCH v. 5 (Edgar 2010) with an identity threshold of 0.85 and compared to the *Myotis lucifugus* draft genome using BLAST v. 2.2.25 (Altschul *et al.* 1990). Clusters that aligned to the same or nearly the same position in the genome were merged. Sequences for each cluster (putative locus) were then aligned using MUSCLE v. 3.8.31 (Edgar 2004). The aligned sequence data were run through a custom script to identify single-nucleotide polymorphisms (SNPs) and insertions/deletions (indels) and to identify the alleles for each sample and locus (DaCosta & Sorenson 2014). We examined alignments for all loci with three or more variable sites in the last five alignment positions, and loci that fell in the tail of the distribution for number of polymorphisms per locus, excluding loci or manually re-aligning sequences as warranted. Loci with missing genotypes for >10% of samples were removed from further analyses.

To summarize rangewide genomic variation, we used principal components analysis (PCA) of the SNP and indel data in the R package *adegenet* v. 1.3-4 (Jombart 2008; R Development Core Team 2010). We replaced missing data at SNP/indel sites in the PCA with the mean frequency of the given allele across all samples. To measure the correlation between genetic and geographic distances between populations/sampling sites, we calculated pairwise Φ_{ST} values for sites with ≥4 individuals using a custom Python script for a sample of 716 RAD loci at which genotypes were successfully scored in all rangewide samples. All Φ_{ST} estimates were based on pairwise nucleotide differences between sequences (Excoffier *et al.* 1992). Nucleotide diversity for each population was also estimated from these loci using the Python script. Statistical significance of the correlation between genetic and geographic distances was tested by the Mantel test using MANTELPIECE v. 1.0 in R (R Development Core Team 2010; Postma 2011).

The rangewide analysis included eastern samples collected from maternity colonies, swarming sites, hibernating colonies and foraging sites, whereas western samples were collected only from maternity colonies and foraging sites because the locations of few hibernacula in western North America are known (see Results for a delineation of 'eastern' and 'western'; Table S1, Supporting information). In some bat species, female philopatry

© 2015 John Wiley & Sons Ltd

1365294x, 2015, 22, Downloaded from https://onlinelibrary.wiley.com/doi/10.1111/mec.13396, Wiley Online Library on [19/11/2022]. See the Terms and Conditions (https://onlinelibrary.wiley.com/terms-and-conditions) on Wiley Online Library for rules of use; OA articles are governed by the applicable Creative Commons License

to natal maternity colonies leads to greater mitochondrial structure among maternity colonies than among swarming sites at hibernacula, where individuals from many maternity colonies gather to mate (Kerth *et al.* 2000, 2002; Veith *et al.* 2004). Conversely, if there is fidelity to swarms and hibernacula, mating in swarms at hibernacula should result in greater autosomal structure among hibernacula. To test for potential biases resulting from differences in sampling between regions, we tested for differences in structure between maternity colonies, hibernacula and foraging sites. We plotted Φ_{ST} against geographic distance for each capture site type for RAD and mtDNA sequence data, respectively (Fig. S1; see Table S1, Supporting information, for sample sizes and site types). We found no significant differences in slopes between hibernacula, maternity colonies and foraging sites for RADs or for mtDNA in the eastern region (all $P > 0.109$; Fig. S1B,D, Supporting information), or between maternity colonies and foraging sites in the western region (all $P > 0.738$; Fig. S1A,C, Supporting information). Likewise, comparisons of structure between western maternity colonies and eastern maternity colonies were essentially identical to comparisons of western maternity colonies and eastern hibernacula (Fig. S2, Supporting information). These findings are consistent with population genetic and mark–recapture studies of *M. lucifugus*, which found relatively high rates of female dispersal among maternity colonies, hibernacula and swarming sites (Dixon 2011a; Norquay *et al.* 2013; Burns *et al.* 2014), suggesting that philopatry to natal maternity colonies is not sufficient to cause significant differences in population structure among site types. In addition, the 'sampling location error' generated by seasonal dispersal and sampling at different times of year should be small relative to the size of the continent in a broad-scale assessment of continental population structure. Thus, samples from all site types were analysed together when assessing continental genetic structure.

To measure genetic differentiation among the 14 hibernating colonies within the WNS-affected region for the WNS spread model, we generated RAD-seq data for 62 samples and sequenced cyt*b* for 128 samples. We used 871 RAD loci at which genotypes were successfully scored in all samples and calculated pairwise Φ_{ST} values between colonies using a custom Python script. For cyt*b*, pairwise Φ_{ST} values were calculated in ARLEQUIN v. 3.5 (Excoffier *et al.* 2005). We tested the correlation between Φ_{ST} and geographic distance among colonies using MANTELPIECE in R (Postma 2011).

WNS spread model

The appearance of WNS in bats is mainly restricted to the hibernating season (Blehert *et al.* 2009; Langwig *et al.* 2015), and thus, we modelled disease spread to uninfected (i.e. susceptible) colonies as a yearly, binomial response using mixed-effects logistic regression models. We used a logit link in the function *lmer* from the *lme4* package in R (R Development Core Team 2010; Bates *et al.* 2011). During each year of the epizootic (2008–2014), colonies either remained susceptible (0) or became infected (1); colonies transitioned from susceptible to infected in the first year that WNS was reported as suspected or confirmed for the county in which the colony was located (USFWS 2015). Once infected, a colony became a potential source of infection for susceptible colonies in subsequent years. Because we lacked samples for the colony with the first known cases of WNS (Howes Cave, NY, USA; Blehert *et al.* 2009), our data begin in 2008 with a mine complex in Ulster County, NY, USA, as the source of infection because it is the geographically closest site to Howes Cave in our sample.

We reasoned that neighbouring or well-connected infected colonies should contribute most heavily to infection risk at a susceptible colony, whereas distant and genetically differentiated colonies should contribute little. Thus, we measured the connectivity of a given susceptible colony to infected colonies in two ways: (i) as the genetic differentiation (Φ_{ST}) and the geographic distance, respectively, between a focal susceptible colony and the genetically most similar or geographically closest infected colony (i.e. the genetic and geographic proximity, respectively, to an infected colony); and (ii) considering all infected colonies as potential sources, we calculated 'genetic centrality' and 'geographic centrality' in relation to all infected colonies, a composite measure of connectedness to all infected colonies in the data set. Analogous to a commonly used calculation of the centrality of a node in a network (Opsahl *et al.* 2010), geographic centrality for a susceptible colony was calculated as the sum of reciprocals of geographic distances to all infected colonies. The centrality calculation incorporates distance information from all potential infected source colonies to a given susceptible colony, so that proximate infected colonies are weighted heavily, and distant infected colonies make smaller contributions to the measurement. Genetic centrality for a susceptible colony in relation to infected colonies was similarly calculated as the sum of reciprocals of Φ_{ST} + median Φ_{ST}, with the median RAD or cyt*b* Φ_{ST} value in the denominator to accommodate Φ_{ST} values of zero (see Fig. S3, Supporting information for a more detailed description).

We set the lower bound at zero for all Φ_{ST} estimates. Covariates were standardized to have a mean of zero and variance of one. To avoid highly correlated independent variables, we evaluated sets of models using

© 2015 John Wiley & Sons Ltd

1365294x, 2015, 22, Downloaded from https://onlinelibrary.wiley.com/doi/10.1111/mec.13396, Wiley Online Library on [19/11/2022]. See the Terms and Conditions (https://onlinelibrary.wiley.com/terms-and-conditions) on Wiley Online Library for rules of use; OA articles are governed by the applicable Creative Commons License

'centrality covariates' (*centDistance*, *centCytb* Φ_{ST} and *centRAD* Φ_{ST}) as fixed effects separately from models using 'proximity covariates' (*Distance*, *cytb* Φ_{ST} and *RAD* Φ_{ST}) as fixed effects. *Year* (random intercept) and *Site* (random intercept) were considered as random effects. We first selected random effect terms by comparing AIC_C scores of full models (i.e. models with all fixed centrality or proximity covariates), varying only random effects (Zuur *et al.* 2009). We evaluated conditional modes and posterior variances of each random effect in each model for deviations from zero, which would suggest that a given random effect captures variation and warrants inclusion in the model (Bates 2010). After excluding unnecessary random effects, we then evaluated candidate models that included the retained random effect(s), varying fixed effects only. We evaluated all possible permutations of the fixed effects in each full model (centrality covariates or proximity covariates, analysed separately) and ranked them by AIC_C using the *dredge* function in R (Burnham & Anderson 2004; Barton 2011). Model fits were evaluated using the Hosmer–Lemeshow *c* statistic and AUC in the R package *pROC* (Hosmer *et al.* 1997).

Results

Genetic structure and WNS spread in eastern North America

Among hibernating colonies in the WNS-affected region within eastern North America, genetic differentiation at the mitochondrial cytochrome *b* (cyt*b*) gene was variable (Φ_{ST} = 0.215, $P < 0.0001$; range = ~0–0.537; significance based on 10 100 permutations of the data), whereas differentiation at nuclear RAD loci was generally lower (Φ_{ST} = 0.008, $P < 0.0001$; range ~0–0.045). Genetic differentiation was weakly correlated with geographic distance for cyt*b* (Pearson r^2 = 0.112, Mantel test, P = 0.012), but the small correlation coefficient indicates substantial variation in Φ_{ST} not accounted for by geographic distance. Differentiation at RAD loci was not correlated with geographic distance (Pearson r^2 = 0.004, Mantel test, P = 0.296), and Φ_{ST} values for cyt*b* and RAD loci were also not significantly correlated (Pearson r^2 = 0.025, Mantel test, P = 0.188), suggesting that the geographic distance and the two genetic differentiation covariates in our model of WNS spread were largely independent.

To evaluate the relationship between genetic differentiation and WNS spread, we used mixed-effects, logistic regression models of WNS incidence among hibernating bat colonies in the WNS-affected region of eastern North America. The variance estimates for levels of the random effect *site* deviated from zero, whereas variance estimates for levels of the random effect *year* did not deviate from zero, suggesting that between-year variation was not sufficient to warrant incorporating it as a random effect in the models (Bates 2010). In addition, AIC_C scores indicate that model fit did not improve when *year* was included as a random effect (Table S2, Supporting information); thus, *site* was retained as the sole random effect in all candidate models.

The best model using centrality covariates (which included *centCytb* Φ_{ST} as the only fixed effect) fit the data only slightly better than the null model (null model ΔAIC_C = 2.07; Table S3, Supporting information); thus, we focus below only on models using the proximity covariates for genetic and geographic distance. Consistent with our hypotheses, estimated coefficients were negative for both genetic differentiation and geographic distance in all WNS risk models (Table 1). The full model, including *Distance*, *RAD* Φ_{ST} and *cytb* Φ_{ST}, best explained WNS risk relative to all other candidate models (ΔAIC_C = 0; weight = 0.63; Table 1). The model lacking genetic covariates altogether (*Distance* as the sole fixed effect) was substantially worse at explaining the data (ΔAIC_C = 6.70; weight = 0.02; likelihood ratio test P = 0.003). Although sample sizes used to estimate RAD Φ_{ST} were low for some hibernacula (Table S1, Supporting information), the large number of RAD loci should provide reasonably robust estimates of Φ_{ST}. When sites with $n < 4$ individuals (eight alleles) were excluded from the data set, the model ranks remained identical and the full model was significantly better than the model with geographic distance only. The Hosmer–Lemeshow *c* statistic was nonsignificant (χ^2 = 3.08, P = 0.929), and the area under the curve (AUC) for the best model was high (AUC = 0.980), both suggesting that the model provided a good fit to the data. Models that included genetic covariates captured observed heterogeneity in the spatial spread of WNS, including the rapid southward spread early in the epizootic and delayed westward spread, generally reflecting the higher differentiation between hibernacula across the Appalachians relative to hibernacula along the eastern Appalachians (Fig. 1). For example, in 2009–2010, a colony in western Pennsylvania that was further from infected sources became WNS positive before colonies that were closer to, but more highly differentiated genetically from infected sources. The same year, a susceptible colony in West Virginia (just west of the southern Appalachians) was within 100 km of an infected colony, but was relatively highly differentiated at RAD loci from infected colonies, and thus was predicted to have low WNS risk. Conversely, the presumably high connectivity of colonies along the eastern Appalachians, which are characterized by low levels of genetic differentiation, may have facilitated the southward spread of WNS in 2008–2009 (Fig. 1).

© 2015 John Wiley & Sons Ltd

1365294x, 2015, 22, Downloaded from https://onlinelibrary.wiley.com/doi/10.1111/mec.13396, Wiley Online Library on [19/11/2022]. See the Terms and Conditions (https://onlinelibrary.wiley.com/terms-and-conditions) on Wiley Online Library for rules of use; OA articles are governed by the applicable Creative Commons License

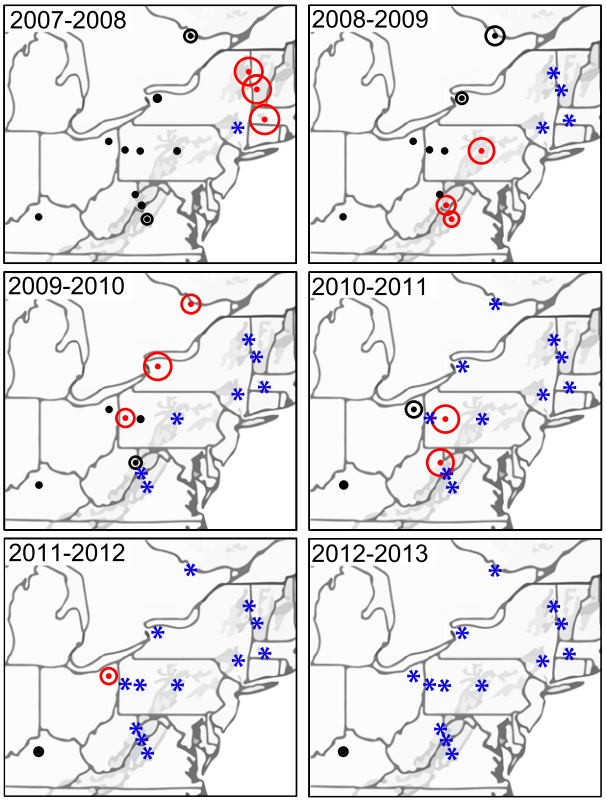

Fig. 1 Fitted yearly probabilities of white-nose syndrome among hibernating bat colonies for the top model (*Distance + RAD* Φ_{ST} + *Cytb* Φ_{ST}; $\Delta AIC_C = 0$). Blue asterisks are previously infected source colonies; red points are susceptible colonies that became infected in the year indicated; black points are susceptible colonies that had not yet become infected. Sizes of open circles surrounding each point correspond to the predicted probability of infection in the colony. Grey shading indicates topography of the Appalachian Mountains. In the final year (2013–2014; not shown), fitted probabilities did not change because there were no new infections among the sampled locations.

Genetic structure of the continental little brown myotis population

Across the continent, we find substantial diversity and geographic structure in little brown myotis cyt*b* sequences. Four divergent *Myotis lucifugus* mitochondrial lineages have distinct but partially overlapping geographic distributions (Fig. 2). A widely distributed and highly diverse eastern clade (red and pink in Fig. 2) predominates east of the Rocky Mountains and appears to have expanded into some western populations. A large number of low frequency haplotypes are derived from the most common lineage in the eastern clade, in a star-like pattern indicative of population expansion (shown in red; Slatkin & Hudson 1991). All bats sampled east of the Appalachian Mountains had haplotypes within this sublineage, resulting in significant differences in mtDNA haplotype frequencies across the eastern region. Geographic structure is substantially greater in the west, however, with one clade restricted to the west coast of North America (shown in blue), another restricted to western Montana, Wyoming, Colorado and Utah (green), and another present in northwestern Montana, Saskatchewan, British Columbia and the Yukon (orange). Finally, cyt*b* sequences from three 'long-eared' *Myotis* species (*M. evotis*, *M. thysanodes* and *M. keenii*) fall within the haplotype network for *M. lucifugus* (shown in grey in Fig. 2A), a result consistent with previous findings (Carstens & Dewey 2010).

Nuclear RAD-seq loci were also highly polymorphic. The final set of 4783 RAD loci had an average of one polymorphism per 5.7 base pairs (bp) and 24.9 unique haplotypes (alleles) per locus among the 308 little brown myotis that we sampled across the continental range. PCA of ~84 000 SNPs summarizes genomewide variation across North America (Fig. 3), indicating relatively minimal differentiation among eastern little brown myotis extending from the East Coast to Ontario, Minnesota, Iowa and Missouri (shown in black in Fig. 3). Genetic differentiation of populations increases markedly beginning in North Dakota and Manitoba and moving westwards. Based on these results, the analyses below define the 'eastern region' as including sites from the East Coast to Missouri, Iowa, Minnesota and eastern Ontario (shown in black in Fig. 3), and the 'western region' as all sites further to the west (shown in colours in Fig. 3). West of the Great Plains, the positions of populations along the first two principal component axes roughly approximate a map of their geographic locations, much as has been observed for human populations in Europe (Novembre *et al.* 2008). This result is consistent with a correlation between genetic and geographic distance across the landscape. Topography, however, also influences the genetic structure of little brown myotis populations; for example, MT2, just west of the Front Range of the Rockies, clusters more closely with BC1, 550 km to the west, rather than with AB2 or SK1, 250 km to the north and 300 km to the east, respectively (Fig. 3). For sites west of Minnesota and Ontario, Φ_{ST} and geographic distance were significantly correlated (Mantel test, $r^2 = 0.324$, $P < 0.001$; coloured points, Fig. 3), whereas this relationship was nonsignificant for populations to the east (Mantel test, $r^2 < 0.001$, $P = 0.476$; black points). Over the entire eastern region, Φ_{ST} was low (mean $\Phi_{ST} = 0.007$), never exceeding 0.033 despite distances of up to 2400 km separating sites. Over similar distances in the western region, Φ_{ST} values were generally higher (mean $\Phi_{ST} = 0.055$) and ranged up to 0.195 (AK1 vs. ND1). The Φ_{ST} value for two sites separated by <350 km in western North Dakota and eastern Montana

© 2015 John Wiley & Sons Ltd

1365294x, 2015, 22, Downloaded from https://onlinelibrary.wiley.com/doi/10.1111/mec.13396, Wiley Online Library on [19/11/2022]. See the Terms and Conditions (https://onlinelibrary.wiley.com/terms-and-conditions) on Wiley Online Library for rules of use; OA articles are governed by the applicable Creative Commons License

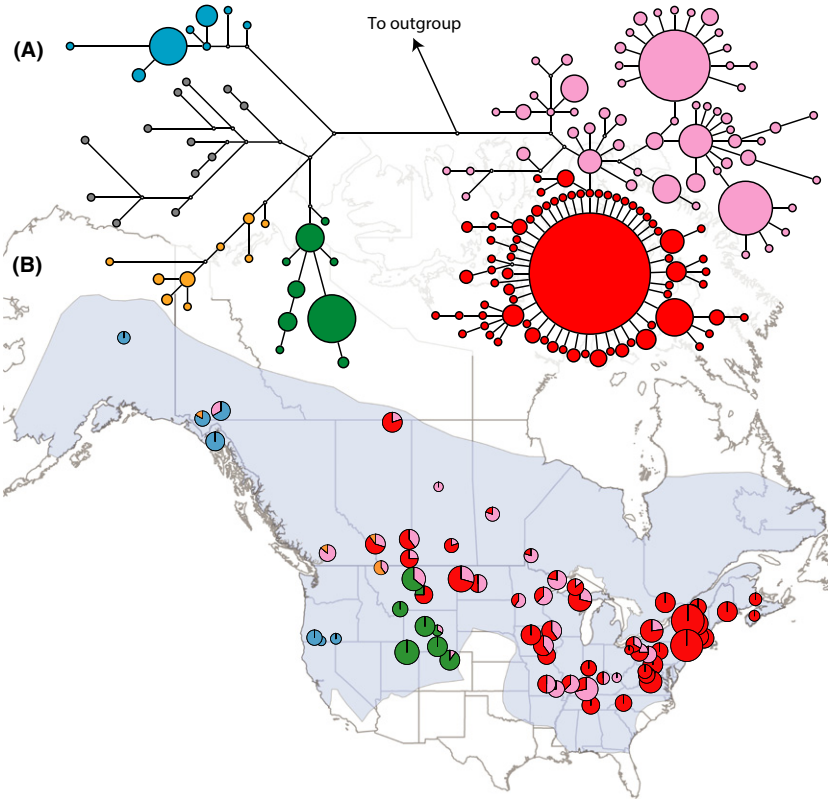

Fig. 2 (A) Cytochrome *b* haplotype network. Circles represent unique haplotypes, with area proportional to the number of bats sharing a haplotype. Line segments are proportional to the number of nucleotide changes, with the shortest branches representing a single change. The arrow indicates the connection to additional out-group samples in a rooted tree. Open circles represent intermediate, unsampled haplotypes. Grey circles represent three 'long-eared' *Myotis* species (*M. evotis*, *M. keenii* and *M. thysanodes*). (B) Cytochrome *b* haplotype frequencies for little brown myotis at capture locations. Pie sizes correspond to the number of bats sampled at each site with colours corresponding to haplotypes as coloured in (A). The range of little brown myotis is shown in blue.

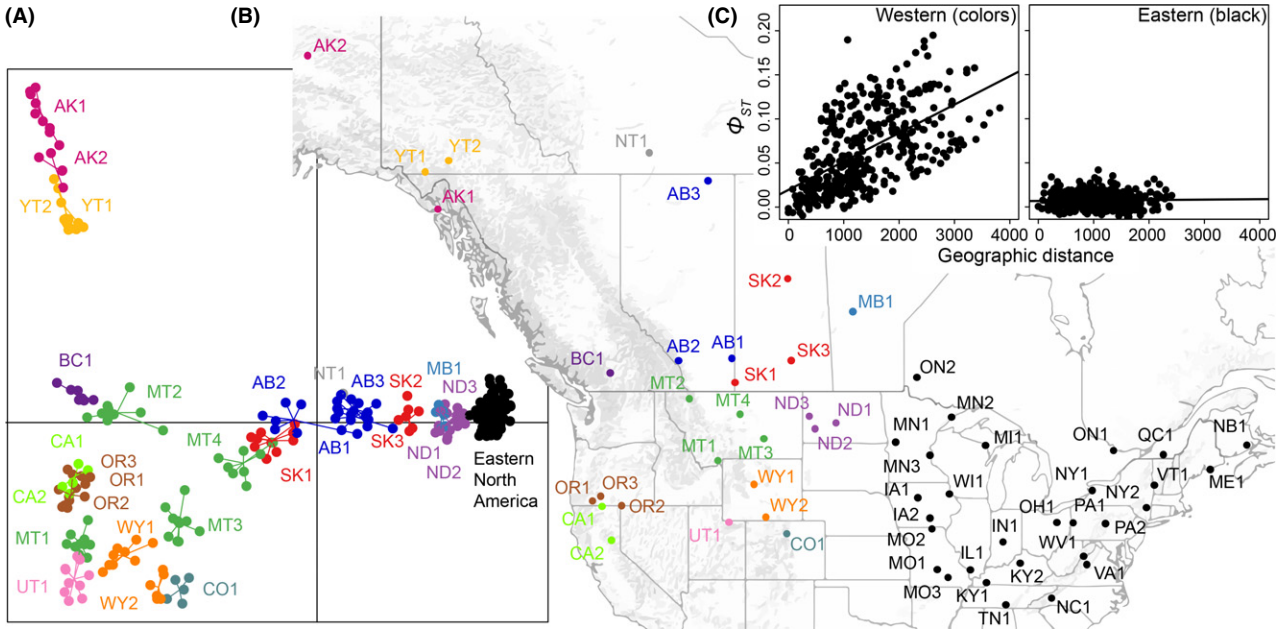

Fig. 3 (A) First and second principal components (PC) scores for individual bats based on RAD-seq data. PC1 and PC2 (*x* and *y* axes, respectively) accounted for 2.12% and 0.61% of the total genetic variance, respectively. Meaningful groupings of samples were not evident in plots of PC axes 3 through 10. Lines join points to the mean PC coordinate for a given capture site. Colours and labels indicate capture sites in (B). (B) Capture sites, coloured and labelled by political boundaries. Grey shading indicates topography, with the Rocky Mountains, Sierra Nevadas and Cascades in western North America, and the Appalachian Mountains in eastern North America. (C) Φ_{ST} values vs. geographic distance between pairs of capture locations in western (coloured points in (B); $P < 0.001$), and eastern North America (black points in B; $P = 0.476$).

© 2015 John Wiley & Sons Ltd

1365294x, 2015, 22, Downloaded from https://onlinelibrary.wiley.com/doi/10.1111/mec.13396, Wiley Online Library on [19/11/2022]. See the Terms and Conditions (https://onlinelibrary.wiley.com/terms-and-conditions) on Wiley Online Library for rules of use; OA articles are governed by the applicable Creative Commons License

Table 1 Mixed logistic regression models of white-nose syndrome (WNS) risk from 2008 through 2014 based on geographic and genetic proximity (distance and Φ_{ST}, respectively) of susceptible colonies to an infected colony in the WNS-affected region of eastern North America

Model	Intercept	Distance	RAD Φ_{ST}	Cyt*b* Φ_{ST}	d.f.	logLik	AICc	ΔAICc	Weight
1	−5.23*	−3.16*	−5.52*	−4.91	5	−13.49	38.8	0.00	0.63
2	−2.08*	−2.16*	−3.23*		4	−16.26	41.7	2.89	0.15
3	−2.16*	−1.23*		−2.89^	4	−16.48	42.2	3.32	0.12
4	−2.40^		−1.84	−3.51^	4	−17.57	44.3	5.50	0.04
5	−1.71^			−2.72^	3	−18.93	44.6	5.72	0.04
6	−1.02*	−1.29*			3	−19.42	45.5	6.70	0.02
7	−0.96^		−1.39		3	−21.77	50.2	11.39	0.00
8	−0.77*				2	−23.70	51.7	13.89	0.00
Model Avg.	−4.05	−2.49^ (0.92)	−4.04^ (0.83)	−3.68 (0.82)					

Coefficients for standardized covariates are presented. The intercept represents the log odds of infection when all standardized coefficients are zero (i.e. mean unstandardized values, equivalent to an infection probability of 0.005 for the top model). Model averaged coefficients with shrinkage are presented in the last row, with covariate weight shown in parentheses. Capture site was included as a random effect in all models. *$P < 0.05$; ^$P < 0.10$.

(Φ_{ST} = 0.058; ND3 vs. MT3), for example, was greater than the maximum level of differentiation observed for all comparisons in the eastern region (Φ_{ST} = 0.033). Genomewide nucleotide diversity within sampling sites ranged from 0.0088 to 0.0111 (Table S4, Supporting information) and was significantly higher for sites in the western region (mean = 0.0102) than the eastern region (mean = 0.00947; *t*-test, $P < 0.0001$).

Discussion

The significant relationship between little brown myotis population genetic structure and the spread of WNS within the current geographic extent of the expanding epizootic is consistent with a coupling of pathogen introduction and host dispersal. Reflecting historical patterns of gene flow, genetic differentiation among host populations may serve as a useful proxy for host dispersal in spatially explicit models of disease spread. We are not aware of previous studies quantitatively linking host population genetic structure to temporal observations of disease emergence across the landscape and using the estimated connectivity of host populations to provide a prospective assessment of future invasion to new regions.

Although little brown myotis is just one of seven bat species known to be infected by *Pseudogymnoascus destructans*, it is probably an important driver of WNS spread because of the following reasons: (i) it has the highest prevalence and loads of the fungal pathogen throughout hibernation among known host species, with nearly 100% of individuals infected at the onset of the hibernation period (Langwig *et al.* 2015); (ii) it is abundant, highly aggregated and densely distributed in hibernacula (Humphrey & Cope 1976; Brack 2007; Frick *et al.* 2010; Wilder *et al.* 2011; Langwig *et al.* 2012), particularly in the north-eastern United States where it comprises nearly 90% of individuals in a typical hibernaculum (Wilder *et al.* 2011). Because of its high abundance in hibernacula and susceptibility to WNS, little brown myotis account for most *P. destructans* infections, such that opportunities for pathogen dispersal by other hosts are far less frequent; (iii) its presence in winter colonies is associated with increased risk of WNS (Wilder *et al.* 2011). The significant correlation between WNS spread and population connectivity in eastern North America provides further evidence of the historical importance of little brown myotis in pathogen dispersal in the WNS-affected region. There are 25 hibernating bat species across North America that may be vulnerable to infection by the cold-growing fungus (Blehert *et al.* 2009; Turner *et al.* 2011), but none are known to be so heavily infected, widely distributed and abundant as little brown myotis (IUCN 2015). Thus, this species has likely been and may continue to be the dominant host species driving WNS spread across much of the continent.

In eastern North America, little brown myotis mate in swarms in the fall at the cave or mine in which they hibernate during the winter (Humphrey & Cope 1976; Norquay *et al.* 2013). Following emergence from hibernation in the spring, bats disperse and females may travel up to hundreds of kilometres from their hibernaculum to a maternity colony (Davis & Hitchcock 1965). Fungal loads, and consequently the potential for transmission, are highest during hibernation and drop to undetectable levels over the summer in surviving bats, suggesting that dispersal between hibernacula (as opposed to other seasonal sites) is most likely to result in spread of the pathogen (Langwig

© 2015 John Wiley & Sons Ltd

1365294x, 2015, 22, Downloaded from https://onlinelibrary.wiley.com/doi/10.1111/mec.13396, Wiley Online Library on [19/11/2022]. See the Terms and Conditions (https://onlinelibrary.wiley.com/terms-and-conditions) on Wiley Online Library for rules of use; OA articles are governed by the applicable Creative Commons License

et al. 2015). Because mating and therefore gene flow is associated with swarming at hibernacula (Thomas *et al.* 1979), host population genetic structure among hibernation sites should reflect connectivity relevant to disease spread. Norquay *et al.* (2013) found that approximately 4% of bats banded and recaptured at hibernacula in Ontario and Manitoba were recaptured at different hibernacula in subsequent years. Hibernating colonies in eastern North America are common across the landscape and frequently numbered tens of thousands of little brown myotis before declines from WNS (Culver *et al.* 1999; Frick *et al.* 2010; Wilder *et al.* 2011; Langwig *et al.* 2012), providing opportunities for both gene flow and pathogen dispersal. The minimal population genetic structure in eastern North America (Figs 2 and 3) and the rapid spread of WNS in this region fit expectations based on direct observations of dispersal. Although the seasonal timing of dispersal between hibernacula, which may influence the likelihood of pathogen transmission, remains unknown, the significant relationship with host population structure suggests that historical patterns of dispersal in little brown myotis are relevant to understanding contemporary disease spread.

Genomewide differentiation of little brown myotis populations increases substantially moving westward from North Dakota and Manitoba, where bats from neighbouring sites become increasingly distinguishable in PC plots of SNP data (Fig. 3). Likewise, the geographic distributions of divergent mitochondrial lineages and the strong correlation between genomewide differentiation and geographic distance (Figs 2 and 3) indicate much lower historical connectivity and dispersal among populations in western North America. All bats sampled west of the Great Plains were captured during the summer, either from maternity colonies or foraging sites (Table S1, Supporting information). Given that the genetic structure of western populations mirrors the geography of summer capture locations, it is unlikely that western bats disperse widely to mate in the fall. If autosomal gene flow occurs at hibernacula in western North America, and fidelity to swarming sites and hibernacula is high, as has been shown in the East (Humphrey & Cope 1976; Norquay *et al.* 2013), we expect greater structure among hibernacula than summer sites. Thus, the level of genetic differentiation between geographically proximate summer sites in western North America suggests contrasting patterns of seasonal dispersal and/or mating behaviour between the two regions. Unlike eastern bats, which disperse widely between summer localities and swarming sites/hibernacula (Davis & Hitchcock 1965; Humphrey & Cope 1976), western bats must remain relatively close to swarming sites and hibernacula throughout the year. Available observations west of the Great Plains indicate that little brown myotis over-winter in small groups (singly to dozens of individuals; Perkins *et al.* 1990; Nagorsen *et al.* 1993; Hendricks 2012), suggesting that the large swarms at hibernacula that facilitate high rates of gene flow in eastern North America may be far smaller or altogether absent in the West, resulting in lower connectivity and greater structure among populations.

Our rangewide genomic data suggest that the spread of WNS by an important host is likely to be slower in western North America than in the eastern half of the continent, where a rapid geographic expansion of the disease has been observed over the past 8 years. Given that the spread of WNS to date has been correlated with subtle patterns of genetic differentiation in eastern North America, the rate of dispersal of the fungal pathogen by little brown myotis should decrease as WNS moves into the Great Plains, where genetic differentiation among localities increases substantially. Moreover, a study of winter little brown myotis colonies in central Canada suggests that gene flow moves predominately north-west to south-east, opposing the direction of spread of the pathogen (Davy *et al.* 2015). Winter surveys show that the total numbers of individuals of all species in hibernating colonies are far smaller in western North America (Perkins *et al.* 1990; Nagorsen *et al.* 1993; Hendricks 2012; Weller *et al.* 2014). WNS tends to emerge in larger colonies first, where the probability of pathogen introduction and transmission probably increases with the number of bats entering a hibernaculum (Wilder *et al.* 2011), and thus, emergence of the disease may be further delayed due to smaller winter colonies in western North America. All else being equal, infrequent and locally restricted dispersal among smaller populations should decrease opportunities for spread of the pathogen over the landscape. Moreover, the higher level of nucleotide diversity in western North America may offer greater potential for the evolution of disease resistance based on standing genetic variation.

The prediction above relies on genetic differentiation as a proxy for contemporary patterns of dispersal and connectivity among populations. Genetic differentiation, however, is influenced by a number of factors, including time since divergence, population sizes, bottlenecks and expansions, as well as rates of gene flow over time (Avise 2000; Manel & Holderegger 2013). The genetic similarity of eastern little brown myotis populations is likely due in part to recent postglacial expansion (Dixon 2011b; Burns *et al.* 2014), but direct observations of dispersal in this region are consistent with a high level of contemporary connectivity. In contrast, substantially greater genetic differentiation in western North America would not be expected if rates of dispersal were as high as have been observed in the East. Thus, our data indi-

© 2015 John Wiley & Sons Ltd

1365294x, 2015, 22, Downloaded from https://onlinelibrary.wiley.com/doi/10.1111/mec.13396, Wiley Online Library on [19/11/2022]. See the Terms and Conditions (https://onlinelibrary.wiley.com/terms-and-conditions) on Wiley Online Library for rules of use; OA articles are governed by the applicable Creative Commons License

cate substantial differences in the patterns and geographic extent of both historical and contemporary gene flow between the two regions.

Our qualitative prediction that WNS will spread more slowly in western North America is based primarily on strong evidence of lower historical connectivity of the populations of an important host beyond the current distribution of the disease. The complex topography of western North America probably increases isolation among populations of little brown myotis and probably affects other hibernating bat species in a similar way (Cryan *et al.* 2000; Piksa *et al.* 2011). The emergence of the disease in a susceptible colony, however, depends on a range of factors, including seasonal variability of transmission dynamics, changes in dispersal behaviour of infected bats, bat species community composition and host competency, and environmental conditions, many of which vary across the continent and contribute uncertainty to our prediction (Anderson *et al.* 1992; Altizer *et al.* 2006; Paull *et al.* 2011). For example, as yet unaffected host species may compensate for a reduced rate of pathogen dispersal by little brown myotis in western North America and may drive disease spread outside the range of our focal species. Our predictions are, like any predictions of the future, subject to a range of uncertainties. In addition, we did not find evidence of complete isolation among any of the western little brown myotis populations we sampled. Thus, there is currently no basis for suggesting that western North America will not be affected by WNS.

There are few examples in the literature of studies that quantitatively test the relationship between the genetic structure of a host population and the observed spread of an infectious disease (Biek & Real 2010). Our analysis of eastern populations confirms the relationship between host population structure and WNS risk thus far and provides the basis for a qualitative prediction about the future spread of WNS into western North America by a common host. For expanding infectious diseases, pathogen dispersal by hosts may strongly influence disease dynamics, and predictions of disease spread that assume a homogeneous host population may fail to account for relevant and potentially cryptic breaks and changes in rangewide connectivity (Real & Biek 2007), particularly for widely distributed hosts. Thus, genetic analysis of host population structure may improve predictions of the future dynamics of emerging infectious diseases.

Acknowledgements

We thank the generous researchers and institutions (Table S5, Supporting information) that provided tissue samples or assistance with sample collection, particularly C. Lausen and M. Moore. A. Meyer, M. Meyer and J. Collins assisted with field and laboratory work. J. DaCosta provided invaluable assistance in implementing the ddRAD-seq protocol. P. Buston and C. Schneider offered helpful comments on early versions of the manuscript, and three anonymous reviewers helped to significantly improve the work. Funding was provided by the Morris Animal Foundation, the Woodtiger Fund, Bat Conservation International, and the American Society of Mammalogists.

References

Altizer S, Dobson A, Hosseini P *et al.* (2006) Seasonality and the dynamics of infectious diseases. *Ecology Letters*, **9**, 467–484.

Altschul SF, Gish W, Miller W, Myers EW, Lipman DJ (1990) Basic local alignment search tool. *Journal of Molecular Biology*, **215**, 403–410.

Anderson RM, May RM, Anderson B (1992) *Infectious Diseases of Humans: Dynamics and Control*. Oxford University Press, Oxford.

Archie EA, Luikart G, Ezenwa VO (2009) Infecting epidemiology with genetics: a new frontier in disease ecology. *Trends in Ecology & Evolution*, **24**, 21–30.

Avise JC (2000) *Phylogeography: the History and Formation of Species*. Harvard University Press, Cambridge, Massachusetts.

Baird NA, Etter PD, Atwood TS, *et al.* (2008) Rapid SNP discovery and genetic mapping using sequences RAD markers. *PLoS One*, **3**, e3376.

Balakrishnan CN, Sorenson MD (2007) Dispersal ecology versus host specialization as determinants of ectoparasite distribution in brood parasitic indigobirds and their estrildid finch hosts. *Molecular Ecology*, **16**, 217–229.

Barton K (2011) *MuMIn: Multi-Model Inference. R Package Version 1.0.0*. R Foundation for Statistical Computing, Vienna, Austria.

Bates DM (2010) *lme4: Mixed-effects modeling with R*. URL http://lme4.r-forge.r-project.org/book.

Bates D, Maechler M, Bolker B (2011) Lme4: Linear mixed-effects models using S4 classes.

Biek R, Real LA (2010) The landscape genetics of infectious disease emergence and spread. *Molecular Ecology*, **19**, 3515–3531.

Biek R, Henderson JC, Waller LA, Rupprecht CE, Real LA (2007) A high-resolution genetic signature of demographic and spatial expansion in epizootic rabies virus. *Proceedings of the National Academy of Sciences, USA*, **104**, 7993–7998.

Blanchong JA, Samuel MD, Scribner KT *et al.* (2008) Landscape genetics and the spatial distribution of chronic wasting disease. *Biology Letters*, **4**, 130–133.

Blehert DS, Hicks AC, Behr M *et al.* (2009) Bat white-nose syndrome: an emerging fungal pathogen? *Science*, **323**, 227.

Brack V (2007) Temperatures and locations used by hibernating bats, including *Myotis sodalis* (Indiana bat), in a limestone mine: implications for conservation and management. *Environmental Management*, **40**, 739–746.

Burnham KP, Anderson DR (2004) Multimodel inference – understanding AIC and BIC in model selection. *Sociological Methods & Research*, **33**, 261–304.

Burns LE, Frasier TR, Broders HG (2014) Genetic connectivity among swarming sites in the wide ranging and recently declining little brown bat (*Myotis lucifugus*). *Ecology and Evolution*, **4**, 4130–4149.

© 2015 John Wiley & Sons Ltd

1365294x, 2015, 22, Downloaded from https://onlinelibrary.wiley.com/doi/10.1111/mec.13396, Wiley Online Library on [19/11/2022]. See the Terms and Conditions (https://onlinelibrary.wiley.com/terms-and-conditions) on Wiley Online Library for rules of use; OA articles are governed by the applicable Creative Commons License

Carstens BC, Dewey TA (2010) Species delimitation using a combined coalescent and information-theoretic approach: an example from North American *Myotis* bats. *Systematic Biology*, **59**, 400–414.

Cryan P, Bogan MA, Altenbach JS (2000) Effect of elevation on distribution of female bats in the Black Hills, South Dakota. *Journal of Mammalogy*, **81**, 719–725.

Culver DC, Hobbs HH, Christman MC, Master LL (1999) Distribution map of caves and cave animals in the United States. *Journal of Karst Studies*, **61**, 139–140.

DaCosta JM, Sorenson MD (2014) Amplification biases and consistent recovery of loci in a double-digest RAD-seq protocol. *PLoS One*, **9**, e106713.

Daszak P, Cunningham AA, Hyatt AD (2000) Emerging infectious diseases of wildlife – threats to biodiversity and human health. *Science*, **287**, 443–449.

Davis WH, Hitchcock HB (1965) Biology and migration of the bat, *Myotis lucifugus*, in New England. *Journal of Mammalogy*, **46**, 296–313.

Davy CM, Martinez-Nuñez F, Willis CK, Good SV (2015) Spatial genetic structure among bat hibernacula along the leading edge of a rapidly spreading pathogen. *Conservation Genetics*, **16**, 1013–1024.

Dixon MD (2011a) Population genetic structure and natal philopatry in the widespread North American bat *Myotis lucifugus*. *Journal of Mammalogy*, **92**, 1343–1351.

Dixon MD (2011b) Post-Pleistocene range expansion of the recently imperiled eastern little brown bat (*Myotis lucifugus lucifugus*) from a single southern refugium. *Ecology and Evolution*, **1**, 191–200.

Edgar RC (2004) MUSCLE: multiple sequence alignment with high accuracy and high throughput. *Nucleic Acids Research*, **32**, 1792–1797.

Edgar RC (2010) Search and clustering orders of magnitude faster than BLAST. *Bioinformatics*, **26**, 2460–2461.

Excoffier L, Smouse PE, Quattro JM (1992) Analysis of molecular variance inferred from metric distances among DNA haplotypes: application to human mitochondrial DNA restriction data. *Genetics*, **131**, 479–491.

Excoffier L, Laval G, Schneider S (2005) Arlequin ver. 3.0: an integrated software package for population genetics data analysis. *Evolutionary Bioinformatics Online*, **1**, 47–50.

Frick WF, Pollock JF, Hicks AC *et al.* (2010) An emerging disease causes regional population collapse of a North American bat species. *Science*, **329**, 679–682.

Girard JM, Wagner DM, Vogler AJ *et al.* (2004) Differential plague-transmission dynamics determine *Yersinia pestis* population genetic structure on local, regional, and global scales. *Proceedings of the National Academy of Sciences, USA*, **101**, 8408–8413.

Hendricks P (2012) Winter records of bats in Montana. *Northwestern Naturalist*, **93**, 154–162.

Holmes EC (2004) The phylogeography of human viruses. *Molecular Ecology*, **13**, 745–756.

Hosmer DW, Hosmer T, le Cessie S, Lemeshow S (1997) A comparison of goodness-of-fit tests for the logistic regression model. *Statistics in Medicine*, **16**, 965–980.

Humphrey SR, Cope JB (1976) *Population Ecology of the Little Brown Bat, Myotis lucifugus, in Indiana and North-Central Kentucky*. American Society of Mammalogists, Stillwater, Oklahoma.

IUCN (2015) *The IUCN Red List of Threatened Species*. Version 2015-3. http://www.iucnredlist.org. Accessed on 15 April 2015.

Jombart T (2008) adegenet: a R package for the multivariate analysis of genetic markers. *Bioinformatics*, **24**, 1403–1405.

Kerth G, Mayer F, König B (2000) Mitochondrial DNA (mtDNA) reveals that female Bechstein's bats live in closed societies. *Molecular Ecology*, **9**, 793–800.

Kerth G, Mayer F, Petit E (2002) Extreme sex-biased dispersal in the communally breeding, nonmigratory Bechstein's bat (*Myotis bechsteinii*). *Molecular Ecology*, **11**, 1491–1498.

Langwig KE, Frick WF, Bried JT *et al.* (2012) Sociality, density-dependence and microclimates determine the persistence of populations suffering from a novel fungal disease, white-nose syndrome. *Ecology Letters*, **15**, 1050–1057.

Langwig KE, Frick WF, Reynolds R *et al.* (2015) Host and pathogen ecology drive the seasonal dynamics of a fungal disease, white-nose syndrome. *Proceedings of the Royal Society of London B: Biological Sciences*, **282**, 20142335.

Lorch JM, Meteyer CU, Behr MJ *et al.* (2011) Experimental infection of bats with *Geomyces destructans* causes white-nose syndrome. *Nature*, **480**, 376–378.

Maher SP, Kramer AM, Pulliam JT *et al.* (2012) Spread of white-nose syndrome on a network regulated by geography and climate. *Nature Communications*, **3**, 1306.

Manel Sp, Holderegger R (2013) Ten years of landscape genetics. *Trends in Ecology & Evolution*, **28**, 614–621.

Miller-Butterworth CM, Vonhof MJ, Rosenstern J, Turner GG, Russell AL (2014) Genetic structure of little brown bats (*Myotis lucifugus*) corresponds with spread of white-nose syndrome among hibernacula. *Journal of Heredity*, **105**, 354–364.

Minnis AM, Lindner DL (2013) Phylogenetic evaluation of *Geomyces* and allies reveals no close relatives of *Pseudogymnoascus destructans*, comb. nov., in bat hibernacula of eastern North America. *Fungal Biology*, **117**, 638–649.

Nagorsen DW, Bryant AA, Kerridge D *et al.* (1993) Winter bat records for British Columbia. *Northwestern Naturalist*, **74**, 61–66.

Norquay KJO, Martinez-Nuñez F, Dubois JE, Monson KM, Willis CKR (2013) Long-distance movements of little brown bats (*Myotis lucifugus*). *Journal of Mammalogy*, **94**, 506–515.

Novembre J, Johnson T, Bryc K *et al.* (2008) Genes mirror geography within Europe. *Nature*, **456**, 98–101.

Opsahl T, Agneessens F, Skvoretz J (2010) Node centrality in weighted networks: generalizing degree and shortest paths. *Social Networks*, **32**, 245–251.

Paull SH, Song S, McClure KM *et al.* (2011) From superspreaders to disease hotspots: linking transmission across hosts and space. *Frontiers in Ecology and the Environment*, **10**, 75–82.

Perkins JM, Barss JM, Peterson J (1990) Winter records of bats in Oregon and Washington. *Northwestern Naturalist*, **71**, 59–62.

Piksa K, Bogdanowicz WÇ, Tereba A (2011) Swarming of bats at different elevations in the Carpathian Mountains. *Acta Chiropterologica*, **13**, 113–122.

Postma E (2011) MantelPiece.R. http://www.erikpostma.net/documents/MantelPiece.R

Puechmaille SJ, Wibbelt G, Korn V *et al.* (2011) Pan-European distribution of white-nose syndrome fungus (*Geomyces destructans*) not associated with mass mortality. *PLoS One*, **6**, e19167.

© 2015 John Wiley & Sons Ltd

1365294x, 2015, 22, Downloaded from https://onlinelibrary.wiley.com/doi/10.1111/mec.13396, Wiley Online Library on [19/11/2022]. See the Terms and Conditions (https://onlinelibrary.wiley.com/terms-and-conditions) on Wiley Online Library for rules of use; OA articles are governed by the applicable Creative Commons License

R Development Core Team (2010) *R: A Language and Environment for Statistical Computing*. R Development Core Team, Vienna, Austria.

Rambaut A, Pybus OG, Nelson MI *et al.* (2008) The genomic and epidemiological dynamics of human influenza A virus. *Nature*, **453**, 615–619.

Real LA, Biek R (2007) Spatial dynamics and genetics of infectious diseases on heterogeneous landscapes. *Journal of the Royal Society, Interface*, **4**, 935–948.

Rioux Paquette S, Talbot B, Garant D, Mainguy J, Pelletier F (2014) Modelling the dispersal of the two main hosts of the raccoon rabies variant in heterogeneous environments with landscape genetics. *Evolutionary Applications*, **7**, 734–749.

Slatkin M, Hudson RR (1991) Pairwise comparisons of mitochondrial DNA sequences in stable and exponentially growing populations. *Genetics*, **129**, 555–562.

Swofford DL (2002) *PAUP*. Phylogenetic Analysis Using Parsimony (*and Other Methods), Version 4.0b10*. Sinauer Associates, Sunderland, Massachusetts.

Thogmartin WE, King RA, Szymanski JA, Pruitt L (2012) Space-time models for a panzootic in bats, with a focus on the endangered Indiana bat. *Journal of Wildlife Diseases*, **48**, 876–887.

Thogmartin WE, Sanders-Reed CA, Szymanski JA *et al.* (2013) White-nose syndrome is likely to extirpate the endangered Indiana bat over large parts of its range. *Biological Conservation*, **160**, 162–172.

Thomas DW, Fenton MR, Barclay RMR (1979) Social behavior of the little brown bat *Myotis lucifugus*. I. Mating behaviour. *Behavioral Ecology and Biology*, **6**, 129–136.

Tian H, Zhou S, Dong L *et al.* (2015) Avian influenza H5N1 viral and bird migration networks in Asia. *Proceedings of the National Academy of Sciences, USA*, **112**, 172–177.

Turner GG, Reeder DM, Coleman JTH (2011) A five-year assessment of mortality and geographic spread of white-nose syndrome in North American bats and a look to the future. *Bat Research News*, **52**, 13–27.

USFWS (2015) http://www.whitenosesyndrome.org/resources/map.

Veith M, Beer N, Kiefer A, Johannesen J, Seitz A (2004) The role of swarming sites for maintaining gene flow in the brown long-eared bat (*Plecotus auritus*). *Heredity*, **93**, 342–349.

Verant ML, Boyles JG, Waldrep W Jr, Wibbelt G, Blehert DS (2012) Temperature-dependent growth of *Geomyces destructans*, the fungus that causes bat white-nose syndrome. *PLoS One*, **7**, e46280.

Warnecke L, Turner JM, Bollinger TK *et al.* (2012) Inoculation of bats with European *Geomyces destructans* supports the novel pathogen hypothesis for the origin of white-nose syndrome. *Proceedings of the National Academy of Sciences, USA*, **109**, 6999–7003.

Weller TJ, Thomas SC, Baldwin JA (2014) Use of long-term opportunistic surveys to estimate trends in abundance of hibernating Townsend's big-eared bats. *Journal of Fish and Wildlife Management*, **5**, 59–69.

Wilder AP, Frick WF, Langwig KE, Kunz TH (2011) Risk factors associated with mortality from white-nose syndrome among hibernating bat colonies. *Biology Letters*, **7**, 950–953.

Zuur AF, Ieno EN, Walker NJ, Saveliev AA, Smith GM (2009) *Mixed Effects Models and Extensions in Ecology with R*. Springer Science+Business Media, New York.

All authors conceived of and designed the study. A.P.W. and T.H.K. obtained samples. A.P.W. and M.D.S. generated and analysed the data and wrote the manuscript.

Data accessibility

Cytochrome *b* sequence data: GenBank accession no. KT694375–KT694938. RAD-seq data: NCBI Sequence Read Archive SRP062003. Table S1 lists SRA accession nos. and locality data for all genotyped samples. Data are archived on Dryad (http://dx.doi.org/10.5061/dryad.v1v13).

Supporting information

Additional supporting information may be found in the online version of this article.

Fig. S1 Pairwise Φ_{ST} estimates vs. geographic distance comparing results for samples collected at maternity colonies, foraging sites and hibernacula in eastern North America (sites shown as black points in Fig. 3) and western North America (coloured points in Fig. 3).

Fig. S2 Relationships of Φ_{ST} vs. geographic distance comparing results for eastern maternity colonies and hibernacula, respectively, vs. western maternity colonies.

Fig. S3 Illustration of genetic centrality calculations.

Table S1 Sample location, season, site type, region, collection date and SRA accession nos. for samples used in the disease spread model and rangewide analysis.

Table S2 Comparison of AIC_C scores of models to select random effect terms.

Table S3 Mixed logistic regression models of WNS risk from 2008 through 2014 based on centrality measures of geographic distance and genetic differentiation (Φ_{ST}) between susceptible colonies and infected colonies in eastern North America.

Table S4 Genomewide nucleotide diversity (π) within sampling sites.

Table S5 Individuals and institutions that provided tissue samples or assistance with sample collection.

© 2015 John Wiley & Sons Ltd

1365294x, 2015, 22, Downloaded from https://onlinelibrary.wiley.com/doi/10.1111/mec.13396, Wiley Online Library on [19/11/2022]. See the Terms and Conditions (https://onlinelibrary.wiley.com/terms-and-conditions) on Wiley Online Library for rules of use; OA articles are governed by the applicable Creative Commons License